

available at [www.sciencedirect.com](http://www.sciencedirect.com)journal homepage: [www.elsevier.com/locate/carbon](http://www.elsevier.com/locate/carbon)

# Visualization and functions of surface defects on carbon nanotubes created by catalytic etching

Wei Xia <sup>a,\*</sup>, Xiuli Yin <sup>b</sup>, Shankhamala Kundu <sup>a</sup>, Miguel Sánchez <sup>a</sup>, Alexander Birkner <sup>b</sup>, Christof Wöll <sup>b</sup>, Martin Muhler <sup>a,\*\*</sup>

<sup>a</sup> Laboratory of Industrial Chemistry, Ruhr-University Bochum, 44780 Bochum, Germany

<sup>b</sup> Lehrstuhl für Physikalische Chemie I, Ruhr-University Bochum, 44780 Bochum, Germany

## ARTICLE INFO

### Article history:

Received 27 April 2010

Accepted 10 September 2010

Available online 18 September 2010

## ABSTRACT

Surface defects were created on carbon nanotubes (CNTs) by catalytic steam gasification or catalytic etching with iron as catalysts. The structure and morphology of the etched CNTs were studied by transmission electron microscopy (TEM) and scanning tunneling microscopy (STM). The electronic structure of the etched CNTs was investigated by ultraviolet photoelectron spectroscopy (UPS). The etched CNTs were treated by nitric acid to obtain oxygen-containing functional groups. The amount and the thermal stability of these groups were studied by temperature-resolved X-ray photoelectron spectroscopy (XPS). Temperature-programmed desorption with ammonia as a probe molecule (NH<sub>3</sub>-TPD) was employed to investigate the interaction of the surface defects with foreign molecules in gas phase. TEM and STM studies disclosed the presence of surface defects especially edge planes on the etched CNTs. Etching of CNTs led to a less pronounced  $p$ - $\pi$  band than the as-is CNTs, as evidenced by UPS studies. The XPS and NH<sub>3</sub>-TPD studies demonstrated that the defects on the CNTs enhanced the reactivity of the exposed surfaces allowing obtaining a higher degree of oxygen functionalization and more active adsorption sites.

© 2010 Elsevier Ltd. All rights reserved.

## 1. Introduction

Carbon nanotubes (CNTs) are very promising materials in heterogeneous catalysis due to their unique properties such as electrical conductivity, mechanical stability and chemical resistance [1–3]. CNTs have been reported as catalyst support for various reactions such as hydrogenation [4,5] and fuel cell catalysis [6]. The application of CNTs improves either the activity or the selectivity as compared to other conventional support materials. Carbon was also used as non-metallic catalyst for reactions like the oxygen reduction in fuel cells and the oxidative dehydrogenation of ethylbenzene to styrene [7–10]. The activity was tentatively attributed to surface

defects, especially to edge planes [11,12]. However, direct experimental evidence for the activity and function of the surface defects was not provided.

The oxidation by HNO<sub>3</sub>, O<sub>2</sub> plasma or other strong oxidizing agents, as it is widely employed for the treatment of CNTs, can introduce oxygen-containing functional groups on the carbon surface [13–18]. These oxidation methods, however, cannot significantly enhance the amount of surface defects such as edge planes, steps, etc. Recently, we have reported the creation of surface defects by the catalytic steam gasification (or catalytic etching) of carbon, where a strong increase of surface defects was detected by Raman spectroscopy and transmission electron microscopy (TEM) [19]. It is expected

\* Corresponding author. Fax: +49 234 32 14115.

\*\* Corresponding author. Fax: +49 234 32 14115.

E-mail addresses: [wei.xia@techem.rub.de](mailto:wei.xia@techem.rub.de) (W. Xia), [muhler@techem.rub.de](mailto:muhler@techem.rub.de) (M. Muhler).

0008-6223/\$ - see front matter © 2010 Elsevier Ltd. All rights reserved.

doi:10.1016/j.carbon.2010.09.025

that the obtained surface defects or etching pits can act as anchoring sites for catalytically active metal nanoparticles, thus improving their resistance to sintering.

In this study, we demonstrate the function of the surface defects created by the catalytic etching. The influence of surface defects on the electronic structure of CNTs has been studied by ultraviolet photoelectron spectroscopy (UPS), and experimental evidence originating from temperature-resolved X-ray photoelectron spectroscopy (XPS) and temperature-programmed desorption of ammonia as a probe molecule ( $\text{NH}_3$ -TPD) reveals that the surface defects are active centers for the adsorption of foreign species, and that the thermal stability of the adsorbates is higher on the defect sites.

## 2. Experimental

### 2.1. Sample preparation

The CNTs (Pyrograf<sup>®</sup> III PR-24-PS) with outer diameters of 50–200 nm were obtained from Applied Sciences Inc. (Ohio, USA). Iron was deposited by chemical vapor deposition from ferrocene or by impregnation with an aqueous solution of ammonium ferric citrate. The etching process was described in detail elsewhere [19]. Briefly, the etching was carried out at 670 °C by introducing water vapor (1 vol.%) to the reactor with the presence of hydrogen (99.9999%, 10 vol.%). After reaction, the coke was burned at 450 °C in diluted oxygen. Finally, the etched sample ( $\text{FeO}_x/\text{CNT}$ ) was treated overnight in 1 M  $\text{HNO}_3$  under continuous stirring at room temperature, and then washed thoroughly, filtered and dried to obtain the etched CNTs (e-CNT). For the XPS and  $\text{NH}_3$ -TPD experiments, both the etched CNTs and as-is CNTs were treated at 800 °C in flowing helium (99.9999%) for 60 min to remove the surface polyaromatics. Subsequently, the CNTs were refluxed in concentrated  $\text{HNO}_3$  at 110 °C for 120 min, washed thoroughly and dried for further applications. The samples are denoted as a-CNT (as-is CNT),  $\text{H}^+$ -a-CNT ( $\text{HNO}_3$ -treated as-is CNT) and  $\text{H}^+$ -e-CNT ( $\text{HNO}_3$ -treated etched CNT).

### 2.2. Characterization

The structure of the nanotubes was studied by TEM (Philips CM 200 FEG). The scanning tunneling microscopy (STM) measurements were carried out using a JSPM-4500S ultra-high vacuum (UHV) combination of a scanning electron microscope (SEM) with a STM (JEOL) operating at a base pressure of  $3 \times 10^{-10}$  mbar. The SEM was operated at electron energies from 0.5 to 12 keV and had a resolution of 7 nm at 12 keV. SEM imaging of the STM tip during an approach allowed us to precisely position the tip on a selected part of the sample within an accessible range of 2 mm  $\times$  2 mm.

XPS measurements were carried out in an UHV set-up equipped with a Gamdata-Scienta SES 2002 analyser. The base pressure in the measurement chamber was  $2 \times 10^{-10}$  mbar. Monochromatic Al  $K\alpha$  (1486.6 eV; 14 kV; 55 mA) was used as incident radiation, and a pass energy of 200 eV was chosen resulting in an energy resolution better than 0.5 eV. Charging effects were compensated using a flood gun. Binding energies were calibrated based on positioning

the main C 1s peak at 284.5 eV. The thermal treatments of the CNTs at different temperatures (117 °C, 307 °C, 447 °C, 597 °C, and 727 °C) were performed in UHV ( $8 \times 10^{-9}$  mbar) for 120 min in the preparation chamber of the XPS set-up, followed by transfer in UHV to the measurement chamber. A helium gas discharge lamp emitting light in the ultraviolet region (He II,  $h\nu = 40.82$  eV) was used for UPS measurements. A lamp current of 100 mA and a pass energy of 20 eV were applied for the measurements. The pressure during the measurement was maintained at  $5 \times 10^{-8}$  mbar. The samples were measured at room temperature. Before the measurements the samples were treated at 80 °C in UHV to remove physisorbed water. The CASA XPS program with a Gaussian-Lorentzian mix function and Shirley background was used to analyze the XP spectra quantitatively. The peak positions for all the samples were reproducible using a fixed Gaussian to Lorentz ratio of 70:30 and fixed FWHMs.

For the  $\text{NH}_3$ -TPD, an infrared detector was employed and calibrated for quantitative measurements. In a typical experiment, 200 mg of the CNTs was loaded into a quartz tube reactor with an inner diameter of 15 mm equipped with a thermocouple inside a close-ended glass capillary, which was embedded in the sample during experiment for temperature control. Both the  $\text{H}^+$ -a-CNT and  $\text{H}^+$ -e-CNT samples were first treated in flowing helium (99.9999%) at 600 °C (heating rate 10 K  $\text{min}^{-1}$ ) for 60 min. After cooling down, the adsorption of  $\text{NH}_3$  (8400 ppm 99.95%  $\text{NH}_3$  in 99.9999% He) was performed for 30 min at 30 °C, followed by purging the reactor with helium for 90 min at the same temperature. The CNTs were then heated from 30 °C to 630 °C at a rate of 10 K  $\text{min}^{-1}$  in a helium flow of 100 ml  $\text{min}^{-1}$  (STP). Simultaneously the  $\text{NH}_3$  concentration was recorded.

## 3. Results and discussion

The etching was performed by exposing Fe-loaded CNTs to  $\text{H}_2\text{O}$  vapor at elevated temperatures, where the reaction occurred at the interface between the iron particles and the carbon support. As a result, the iron nanoparticles were embedded into the walls of the CNTs by chemical etching (Fig. 1a). Except for the etching by gasification reaction, it is believed that several other reactions were involved in this process, including the reverse reaction of gasification leading to coke formation, the oxidation of iron by water, etc. Finally the catalysts were fully deactivated. The sample was shortly exposed to air for decoking before cooling to room temperature. The iron nanoparticles, frequently observed as single crystalline  $\text{Fe}_2\text{O}_3$  with a typical lattice spacing of 0.25 nm, were found to be indented into the walls of the nanotubes (Fig. 1b). After dissolving the iron oxide by acid, the created surface defects were detected by Raman spectroscopy [19]. A TEM image of an etched CNT is shown in Fig. 1c. The destruction of the walls can be seen clearly from the diffraction contrast. The same sample was further studied by scanning tunneling microscopy (STM). Surface defects like steps with exposed edge planes can be observed from the three-dimensional STM image shown in Fig. 2a. The dimensions of the defects were derived from the line profiles in cross-section direction (Fig. 2b) as well as in axial direction (Fig. 2c). The

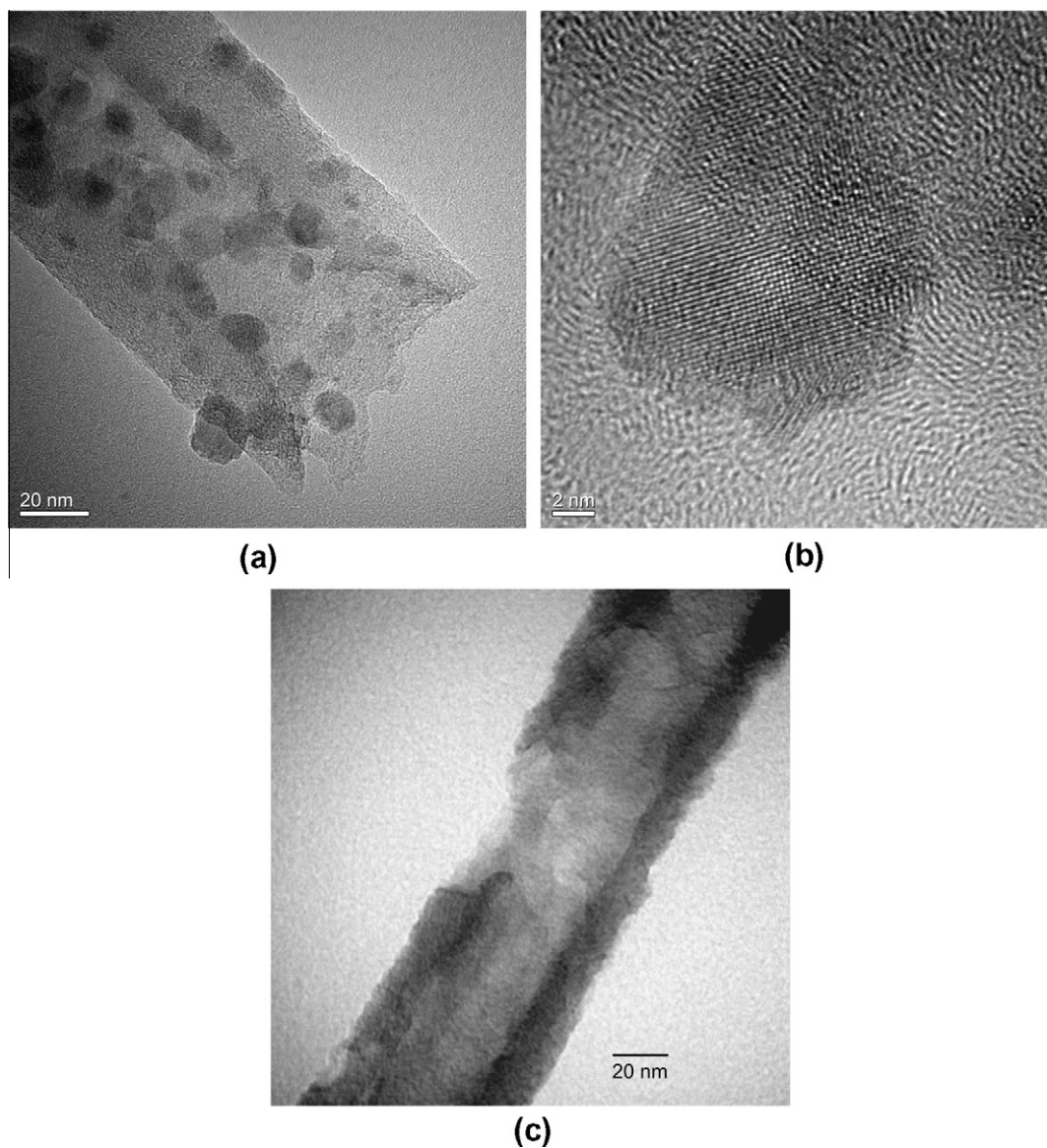


**Fig. 1 – TEM images. (a) Carbon nanotube after catalytic etching using water with iron nanoparticles; (b) Single-crystal iron nanoparticle embedded in the wall of the nanotube; (c) Etched nanotube after the removal of iron.**

presence of etching pits with depths from a few to 10 nm is in good agreement with the TEM observations.

The surface defects on CNTs are supposed to be anchoring points for foreign atoms or chemical moieties, which has been rarely verified experimentally. To confirm this hypothesis, we performed parallel experiments with the etched CNTs and as-is CNTs by employing temperature-resolved XPS and  $\text{NH}_3$ -TPD. To ensure the complete removal of iron used for the etching, a treatment in air (decoking) was performed to remove the coke and expose the iron, followed by overnight washing in acid under continuous stirring. Both the etched CNTs and the as-is CNTs were then purified at 800 °C in flowing helium to remove the surface polyaromatics. Finally, the CNTs were refluxed in concentrated  $\text{HNO}_3$ , washed and dried thoroughly. It is worth to note that in addition to the introduction of oxygen-containing functional groups, the last step of

refluxing in  $\text{HNO}_3$  would have removed any iron residue, if it had been present after the washing overnight.

Carbon, oxygen and nitrogen were detected by XPS, and the survey scans did not show any metallic impurities (Fig. 3). The decomposition and transformation of the oxygen species upon heating was studied based on the O 1s as well as C 1s spectra. The decrease of O 1s peak intensities after thermal treatment at different temperatures in ultra-high vacuum can be seen clearly from the XP spectra shown in Fig. 4. Additionally, the fitting of the peaks provides indications on the thermal stability as well as the transformation of different oxygen species. Hydroxyl groups decompose at relatively lower temperatures. After thermal treatment at 727 °C, the remaining oxygen species are believed to be mainly carbonyls (binding energy ca. 531 eV) and ethers (ca. 533 eV). The oxygen to carbon (O/C) ratio derived from

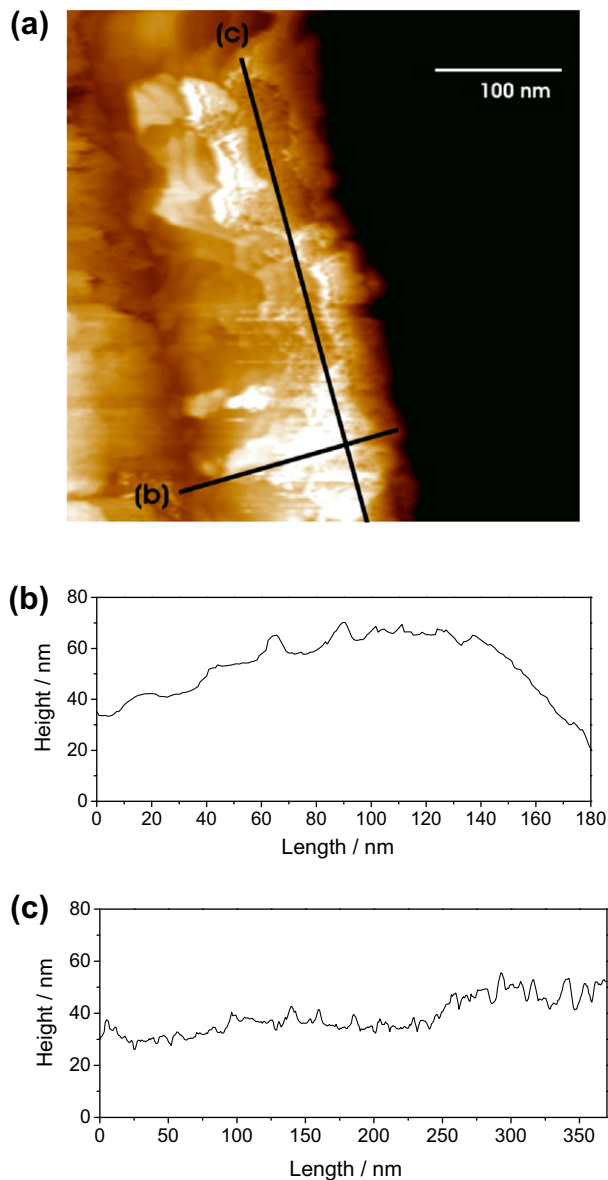


**Fig. 2 – (a) STM image of the defective wall of a nanotube; (b) and (c) line profiles obtained by STM measurement corresponding to the lines marked in (a).**

the XPS surface atomic concentrations [20] is shown in Fig. 5 as a function of the treatment temperatures. It can be seen that the HNO<sub>3</sub>-treated etched CNT sample has a higher amount of oxygen in the whole heating process than the as-is CNTs after HNO<sub>3</sub>-treatment. The as-is CNTs (without HNO<sub>3</sub> treatment) exhibits much less but stable amounts of surface oxygen upon thermal treatments. Both the HNO<sub>3</sub>-treated CNT samples show strong decreases of oxygen upon heating. However, after thermal treatment at 727 °C, the oxygen to carbon ratios of both the HNO<sub>3</sub>-treated samples (etched: 0.060; as-is: 0.046) are still much higher than that of the as-is CNT without HNO<sub>3</sub> treatment (0.017). As indicated by the higher O/C ratios, more oxygen can be anchored on the etched CNTs. The presence of a higher amount of oxygen-containing functional groups at high temperatures

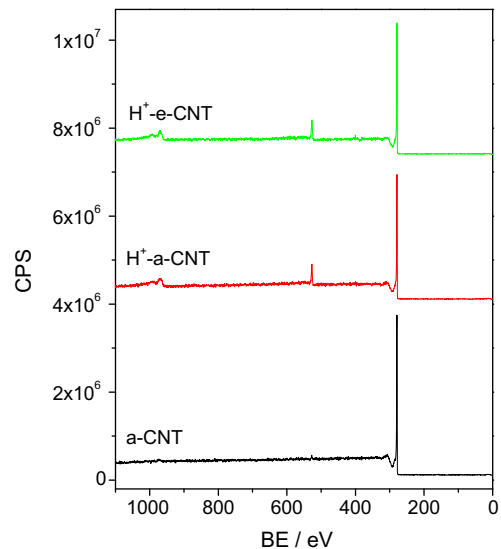


**Fig. 3 – XPS survey spectra of as-is CNT (a-CNT), HNO<sub>3</sub>-treated as-is CNT (H<sup>+</sup>-a-CNT) and HNO<sub>3</sub>-treated etched CNT (H<sup>+</sup>-e-CNT) samples.**

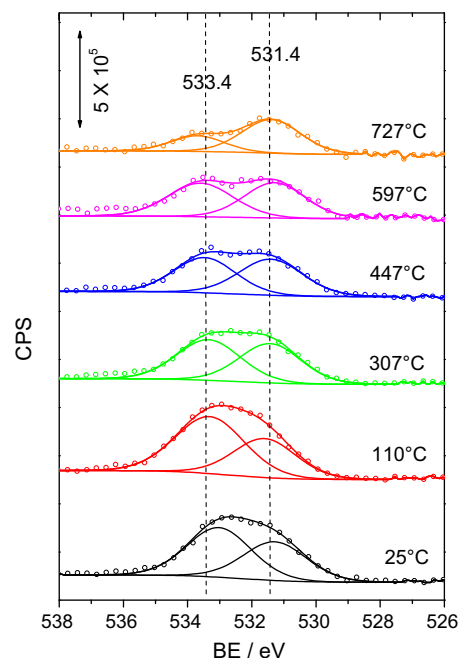


**Fig. 4 – XP O 1s spectra of HNO<sub>3</sub>-treated etched CNTs after pretreatment in the UHV chamber of the XPS setup at different temperatures.**

is of vital importance for catalytic applications of the nanotubes, where heating processes are frequently involved.

It is known from TPD studies that the decomposition of the carboxyl groups occurs at lower temperatures, whereas the phenol, carbonyl and ether groups are more stable and decompose at higher temperatures [21]. The ether-type oxygen between two adjacent graphene layers is presumably the most stable oxygen species on CNTs, which is believed to be one of the major species after thermal treatment at



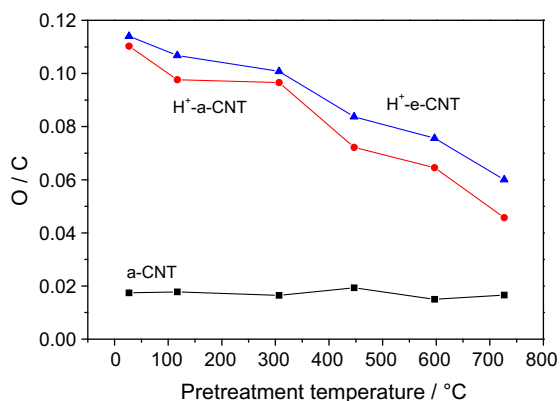


**Fig. 5 – Oxygen to carbon ratio (O/C) as a function of pretreatment temperature of as-is CNTs (a-CNT), HNO<sub>3</sub>-treated as-is CNTs (H<sup>+</sup>-a-CNT) and HNO<sub>3</sub>-treated etched CNTs (H<sup>+</sup>-e-CNT). The O to C ratios were derived from XPS surface atomic concentrations. The pretreatments were carried out in the UHV chamber of the XPS setup.**

727 °C in ultra-high vacuum [22]. Apparently, the presence of surface defects like steps and edge planes facilitates the embedding of oxygen between graphene sheets. Hence the improved thermal stability of oxygen in H<sup>+</sup>-e-CNT can be mainly attributed to the created defects, although the influence of surface area on oxygen amount cannot be fully excluded. Additionally, carbon atoms at defect sites or dangling bonds can also help to anchor the oxygen atoms on the surface.

The presence of surface defects has significant influence on the electronic structure of CNTs [23]. Photoelectron spectroscopy, especially UPS, can provide information about the electronic structure over a wide energy range [24]. Fig. 6 shows the UP spectra of the as-is and etched CNTs excited by He II radiation. The spectra of both samples are dominated by two broad overlapping peaks centered at about 7.7 eV and 3.2 eV, which originate from valence electrons emitted from the p-σ and p-π band, respectively. The changes in the relative peak intensities of the two peaks reflect the structural changes in the samples. It can be seen from Fig. 6 that the etched CNTs have a less pronounced p-π band than the as-is CNTs, which is mainly due to decreasing sp<sup>2</sup> contributions.

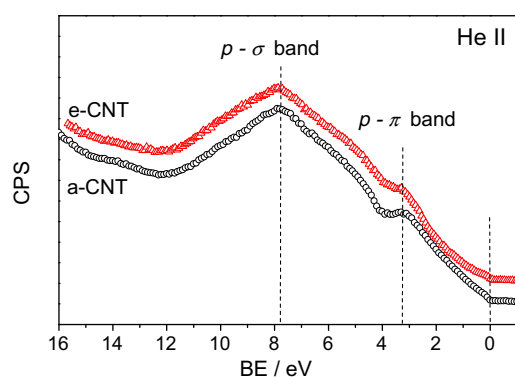


**Fig. 6 – UPS He II spectra of as-is CNTs (a-CNT) and etched CNTs (e-CNT).**

The lowered emission from the π band indicates enhanced structural disorder due to etching, which is in agreement with the results of the XPS and STM studies.

In addition to the XPS and UPS observations, strong evidence on the active role of surface defects was obtained by NH<sub>3</sub>-TPD. It is known that surface acidic groups are the primary adsorption centers, on which ammonia molecules are associated through hydrogen bonds [25]. It is generally accepted that the carboxyl and phenol groups account for the acidic properties of carbon materials [26]. These acidic groups on CNTs decompose below 500 °C in helium [21]. For the NH<sub>3</sub>-TPD measurement, both the HNO<sub>3</sub>-treated CNT samples were first treated in flowing helium at 600 °C. The treatment is believed to be able to remove all the acidic groups, with only basic groups left, which are not active for the adsorption of NH<sub>3</sub>. It can be seen from Fig. 7 that little NH<sub>3</sub> was detected for the as-is CNT sample, whereas much higher amount of NH<sub>3</sub> was identified for the etched CNTs.

The major NH<sub>3</sub> desorption peak was reported to be at about 140 °C for active carbon [27] and activated carbon fibers [28]. Our former studies on HNO<sub>3</sub>-treated CNTs suggested a major NH<sub>3</sub> desorption temperature of 122 °C [29], which is lower than that of active carbon. The difference in desorption temperatures can be related to the apparently stronger acidity of active carbon. However, the major desorption temperature of the etched CNT sample appears at 190 °C, which is at least 50 °C higher than the usually observed temperatures of carbon materials, and about 70 °C higher than the as-is CNT sample. Furthermore, a broad shoulder appears at higher temperatures, which cannot be assigned to a specific adsorption site on the etched surface. The shoulder is believed to be related to different sites that anchor NH<sub>3</sub> strongly on the surface through multiple interactions. It is known that the specific surface area increased after etching. However, the enhanced adsorption of NH<sub>3</sub> cannot be solely interpreted by increased surface areas, since the NH<sub>3</sub> desorption peak shifted to higher temperatures considerably. The higher

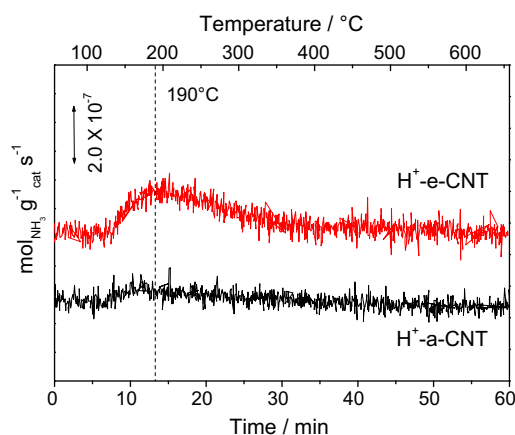


**Fig. 7 – NH<sub>3</sub>-TPD spectra of HNO<sub>3</sub>-treated as-is CNTs (H<sup>+</sup>-a-CNT) and HNO<sub>3</sub>-treated etched CNTs (H<sup>+</sup>-e-CNT). The CNTs were first heat-treated at 600 °C in flowing helium for 60 min before the adsorption of NH<sub>3</sub> at room temperature for 30 min. The spectra were obtained at a heating ramp of 10 K min<sup>-1</sup>.**

desorption temperature clearly indicates enhanced bond strength between  $\text{NH}_3$  and the CNT surface. Additionally, the observed desorption of  $\text{NH}_3$  at 190 °C and higher temperatures cannot originate from the decomposition of nitrogen-containing functional groups like pyridinic or pyrrolic groups on carbon surface. These nitrogen-containing functional groups, which can be created by  $\text{NH}_3$  treatment of carbon at temperatures higher than 200 °C, only decompose at much higher temperatures than 190 °C [30].

Considering the absence of surface acidic groups after heating at 600 °C, and the absence of metallic impurities like Fe species confirmed by XPS, it is assumed that the surface defects are responsible for the uptake of  $\text{NH}_3$ . It is not likely that the residual oxygen species after heating at 600 °C in helium adsorb  $\text{NH}_3$ , otherwise the  $\text{HNO}_3$ -treated as-is CNTs would have showed a stronger  $\text{NH}_3$  desorption peak than it did due to the presence of at least 6.1% (O/C = 0.065) oxygen on the surface as compared to 7.1% (O/C = 0.076) of the  $\text{HNO}_3$ -treated etched CNTs (Fig. 5). Therefore, we can conclude that the surface defects are active sites for the adsorption of  $\text{NH}_3$  presumably at steps and edge planes. The  $\text{NH}_3$ -TPD results are in agreement with the XPS observations supporting the active role of the surface defects.

#### 4. Conclusions

In conclusion, the surface defects of CNTs created by etching were studied by STM and UPS. Edge planes created by etching were visualized, and a less pronounced  $p$ - $\pi$  band was observed for the etched CNTs as compared to as-is CNTs. The adsorption and desorption of chemical moieties on the defect sites was investigated by temperature-resolved XPS and  $\text{NH}_3$ -TPD studies. The created defects on CNTs enhanced the reactivity of the exposed surfaces allowing obtaining a higher degree of oxygen functionalization and more active adsorption sites.

#### Acknowledgement

S. Kundu thanks the Max Planck Society (IMPRS-SurMat) for a research grant.

#### REFERENCES

- [1] de Jong KP, Geus JW. Carbon nanofibers: catalytic synthesis and applications. *Catal Rev-Sci Eng* 2000;42:481–510.
- [2] Serp P, Corrias M, Kalck P. Carbon nanotubes and nanofibers in catalysis. *Appl Catal A* 2003;253:337–58.
- [3] Nhut JM, Pesant L, Tessonnier JP, Wine G, Guille J, Cuong PH, et al. Mesoporous carbon nanotubes for use as support in catalysis and as nanosized reactors for one-dimensional inorganic material synthesis. *Appl Catal A* 2003;254:345–63.
- [4] Planeix JM, Coustel N, Coq B, Bretons V, Kumbhar PS, Dutartre R, et al. Application of carbon nanotubes as supports in heterogeneous catalysis. *J Am Chem Soc* 1994;116:7935–6.
- [5] Yoon B, Wai CM. Microemulsion-templated synthesis of carbon nanotube-supported Pd and Rh nanoparticles for catalytic applications. *J Am Chem Soc* 2005;127:17174–5.
- [6] Girishkumar G, Hall TD, Vinodgopal K, Kamat PV. Single wall carbon nanotube supports for portable direct methanol fuel cells. I. Influence of surface chemical groups. *J Phys Chem B* 2006;110:107–14.
- [7] Maldonado S, Stevenson KJ. Direct preparation of carbon nanofiber electrodes via pyrolysis of iron(II) phthalocyanine: electrocatalytic aspects for oxygen reduction. *J Phys Chem B* 2004;108:11375–83.
- [8] Maldonado S, Stevenson KJ. Influence of nitrogen doping on oxygen reduction electrocatalysis at carbon nanofiber electrodes. *J Phys Chem B* 2005;109:4707–16.
- [9] Pereira MFR, Orfao JJM, Figueiredo JL. Oxidative dehydrogenation of ethylbenzene on activated carbon catalysts. *Appl Catal A* 1999;184:153–60.
- [10] Mestl G, Maksimova NI, Keller N, Roddatis VV, Schlögl R. Carbon nanofilaments in heterogeneous catalysis: an industrial application for new carbon materials? *Angew Chem Int Ed* 2001;40:2066–8.
- [11] Matter PH, Ozkan US. Non-metal catalysts for dioxygen reduction in an acidic electrolyte. *Catal Lett* 2006;109:115–23.
- [12] Keller N, Maksimova NI, Roddatis VV, Schur M, Mestl G, Butenko YV, et al. The catalytic use of onion-like carbon materials for styrene synthesis by oxidative dehydrogenation of ethylbenzene. *Angew Chem Int Ed* 2002;41:1885–8.
- [13] Lakshminarayanan PV, Toghiani H, Pittman Jr CU. Nitric acid oxidation of vapor grown carbon nanofibers. *Carbon* 2004;42:2433–42.
- [14] Banerjee S, Hemraj-Benny T, Wong SS. Covalent surface chemistry of single-walled carbon nanotubes. *Adv Mater* 2005;17:17–29.
- [15] Ajayan PM, Ebbesen TW, Ichihashi T, Iijima S, Tanigaki K, Hiura H. Opening carbon nanotubes with oxygen and implications for filling. *Nature* 1993;362:522–5.
- [16] Tsang SC, Harris PHF, Green MLH. Thinning and opening of carbon nanotubes by oxidation using carbon dioxide. *Nature* 1993;362:520–2.
- [17] Byl O, Liu J, Yates Jr JT. Etching of carbon nanotubes by ozone: a surface area study. *Langmuir* 2005;21:4200–4.
- [18] Kooi SE, Schlecht U, Burghard M, Kern K. Electrochemical modification of single carbon nanotubes. *Angew Chem Int Ed* 2002;41:1353–5.
- [19] Xia W, Hagen V, Kundu S, Wang Y, Somsen C, Eggeler G, et al. Controlled etching of carbon nanotubes by iron-catalyzed steam gasification. *Adv Mater* 2007;19:3648–52.
- [20] Briggs D, Seah MP. Practical surface analysis. England: John Wiley and Sons; 1994. p. 635–8.
- [21] Toebes ML, van Heeswijk JMP, Bitter JH, van Dillen AJ, de Jong KP. The influence of oxidation on the texture and the number of oxygen-containing surface groups of carbon nanofibers. *Carbon* 2004;42:307–15.
- [22] Kundu S, Wang Y, Xia W, Muhler M. Thermal stability and reducibility of oxygen-containing functional groups on multiwalled carbon nanotube surfaces: a quantitative high-resolution XPS and TPD/TPR study. *J Phys Chem C* 2008;112:16869–78.
- [23] Reinke P, Oelhafen P. Thermally induced structural changes in amorphous carbon films observed with ultraviolet photoelectron spectroscopy. *J Appl Phys* 1997;81:2396–9.
- [24] Suzuki S, Watanabe Y, Kiyokura T, Nath KG, Ogino T, Heun S, et al. Electronic structure at carbon nanotube tips studied by photoemission spectroscopy. *Phys Rev B* 2001;63:2454181–7.
- [25] Ellison MD, Crotty MJ, Koh D, Spray RL, Tate KE. Adsorption of  $\text{NH}_3$  and  $\text{NO}_2$  on single-walled carbon nanotubes. *J Phys Chem B* 2004;108:7938–43.
- [26] Montes-Moran MA, Suarez D, Menendez JA, Fuente E. On the nature of basic sites on carbon surfaces: an overview. *Carbon* 2004;42:1219–25.

- 
- [27] Szymanski GS, Grzybek T, Papp H. Influence of nitrogen surface functionalities on the catalytic activity of activated carbon in low temperature SCR of NO<sub>x</sub> with NH<sub>3</sub>. *Catal Today* 2004;90:51–9.
- [28] Grzybek T, Klinik J, Dutka B, Papp H, Suprun V. Reduction of N<sub>2</sub>O over carbon fibers promoted with transition metal oxides/hydroxides. *Catal Today* 2005;101:93–107.
- [29] Xia W, Wang Y, Bergsträsser R, Kundu S, Muhler M. Surface characterization of oxygen-functionalized multi-walled carbon nanotubes by high-resolution X-ray photoelectron spectroscopy and temperature-programmed desorption. *Appl Surf Sci* 2007;254:247–50.
- [30] Arrigo R, Hävecker M, Schlögl R, Su D. Dynamic surface rearrangement and thermal stability of nitrogen functional groups on carbon nanotubes. *Chem Commun* 2008: 4891–3.